



LJMU Research Online

Nelms, MD, Ates, G, Madden, JC, Vinken, M, Cronin, MTD, Rogiers, V and Enoch, SJ

Proposal of an in silico profiler for categorisation of repeat dose toxicity data of hair dyes

<http://researchonline.ljmu.ac.uk/id/eprint/1361/>

Article

Citation (please note it is advisable to refer to the publisher's version if you intend to cite from this work)

Nelms, MD, Ates, G, Madden, JC, Vinken, M, Cronin, MTD, Rogiers, V and Enoch, SJ (2015) Proposal of an in silico profiler for categorisation of repeat dose toxicity data of hair dyes. ARCHIVES OF TOXICOLOGY, 89 (5). pp. 733-741. ISSN 0340-5761

LJMU has developed [LJMU Research Online](#) for users to access the research output of the University more effectively. Copyright © and Moral Rights for the papers on this site are retained by the individual authors and/or other copyright owners. Users may download and/or print one copy of any article(s) in LJMU Research Online to facilitate their private study or for non-commercial research. You may not engage in further distribution of the material or use it for any profit-making activities or any commercial gain.

The version presented here may differ from the published version or from the version of the record. Please see the repository URL above for details on accessing the published version and note that access may require a subscription.

For more information please contact researchonline@ljmu.ac.uk

<http://researchonline.ljmu.ac.uk/>

1 Proposal of an *in silico* profiler for categorisation of repeat dose toxicity data of
2 hair dyes

3 MD Nelms^{1*}, G Ates^{2*}, JC Madden¹, M Vinken², MTD Cronin¹, V Rogiers^{2**}, SJ Enoch^{1**\$}

4

5 ¹School of Pharmacy and Biomolecular Sciences, Liverpool John Moores University, Byrom
6 Street, Liverpool L3 3AF, England.

7 ²Department of Toxicology, Vrije Universiteit Brussel (VUB), Center for Pharmaceutical
8 Research (CePhar), Laarbeeklaan 103, 1090 Brussels, Belgium.

9 *Equally contributing first authors

10 **Equally contributing last authors

11 ^{\$}Corresponding author

12 Dr Steve Enoch

13 E: s.j.enoch@ljmu.ac.uk

14 T: +44(0)151 231 2164

15

16

17 Abstract

18 This study outlines the analysis of repeat dose toxicity data taken from Scientific Committee
19 on Consumer Safety (SCCS) opinions for commonly used hair dyes in the European Union.
20 Structural similarity was applied to group these chemicals into categories. Subsequent
21 mechanistic analysis suggested that toxicity to mitochondria is potentially a key driver of
22 repeat dose toxicity for chemicals within each of the categories. The mechanistic hypothesis
23 allowed for an *in silico* profiler consisting of mechanism-based structural alerts to be
24 proposed. This *in silico* profiler is intended for grouping chemicals into mechanism-based
25 categories within the Adverse Outcome Pathway paradigm.

26 Introduction

27 Significant changes in the European cosmetic and chemical legislations during the last decade
28 have concentrated efforts in the development of alternative methods to animal
29 experimentation for safety testing purposes (Commision, 2003; Commision, 2007). The
30 Adverse Outcome Pathway (AOP) paradigm has emerged as a promising approach in that it
31 enables key events in the pathway that leads to a toxicological outcome to be identified
32 (Ankley *et al.*, 2010; Vinken, 2013; Vinken *et al.*, 2013). Key amongst these events is the
33 Molecular Initiating Event (MIE) which has been the focus for the development of *in silico*
34 profilers (Przybylak and Schultz, 2013). These profilers define the chemical features
35 associated with a given MIE in terms of collections of structural alerts and are intended to be
36 used to categorise chemicals based on a common MIE (Enoch *et al.*, 2011a; Enoch *et al.*,
37 2013a; Enoch and Roberts, 2013; Przybylak and Schultz, 2013; Sakuratani *et al.*, 2013a;
38 Sakuratani *et al.*, 2013b; Vinken, 2013; Vinken, Whelan and Rogiers, 2013). The
39 mechanism-based categories of chemicals that result from such AOP-derived profilers are
40 applicable to predict hazard via read-across and hence assist in the filling of data gaps. In
41 addition, these groupings also form the basis for the more in-depth analysis that is required
42 for an overall risk assessment. In such a situation, additional testing using *in vitro* and/or *in*
43 *chemico* methods to assess other key steps in the AOP is likely to be required. The ability to
44 group chemicals into mechanism-based categories using *in silico* profilers enables advanced
45 testing strategies to be developed based on the prioritisation of chemicals and their testing in
46 the more elaborated and costly assays (Gutsell and Russell, 2013).

47 Repeat dose toxicity results are, however, available for cosmetic ingredients present on the
48 Annexes of Cosmetic Regulation 1223/2009. Indeed, for cosmetic substances for which some
49 concern exists with respect to human health, e.g. colorants, preservatives, UV-filters and hair
50 dyes. These data, consisting of No Observable Adverse Effect level (NOAEL)-values are
51 available through the so-called opinions of the Scientific Committee on Consumer Safety
52 (SCCS) and its predecessors, the Scientific Committee on Cosmetic products and Non-Food
53 Products intended for consumers (SCCNFP) and the Scientific Committee on Consumer
54 Products (SCCP). Clearly, such data could provide a useful starting point for developing
55 MIEs and identifying the chemistry required for the grouping of chemicals for read-across.

56 In particular for hair dyes, high quality toxicological data became available as a consequence
57 of the step-wise strategy of the European Commission to regulate all hair dyes listed as
58 substances in cosmetic products. As such, industry was required to submit safety dossiers for
59 hair dye components and possible mixtures for evaluation by the Scientific Committees. The
60 trigger for this action was the major concern of the scientific community for a putative link
61 between the use of hair dyes and the development of cancer, with a focus on leukaemia and
62 bladder cancer (Gago-Dominguez *et al.*, 2001). Despite the requirement to assess the toxicity
63 of hair dyes, few models or structural alerts for their toxic effects, or rationale for their
64 grouping, is currently available.

65 Therefore, the aim of this study is to propose an *in silico* profiler from the retrospective
66 analysis of the oral repeat dose toxicity data available for hair dyes and retrieved from the
67 Scientific Committees opinions published between 2000 and 2013. Mechanistic information
68 relating these structural alerts to potential MIEs was sought from the peer reviewed literature.

69 Methods

70 *Experimental data*

71 NOAEL values from oral 90-day rat studies for 94 hair dyes were extracted from the opinions
72 of the SCCS and its predecessors between 2000 and 2013. Chemical names, CAS numbers
73 and chemical structures were also taken from these reports. These data were used in the
74 chemoinformatics analysis leading to the development of mechanism-based structural alerts.
75 All data are available as supplementary information in the form of an Excel workbook.

76 *Development of mechanism-based structural alerts*

77 The development of mechanism-based *in silico* profilers suitable for category formation is a
78 time-consuming, literature-intensive process. Previous research leading to the establishment
79 of *in silico* profilers for toxicological endpoints such as skin and respiratory sensitisation
80 utilised a mechanistic hypothesis as a starting point for structural alert development (Enoch *et*
81 *al.*, 2008; Enoch *et al.*, 2012a). However, for complex endpoints such as organ-specific
82 toxicity for which knowledge relating to possible MIEs is lacking, a chemoinformatics
83 approach, coupled with *a posteriori* mechanistic rationalisation, has been shown to be successful
84 (Hewitt *et al.*, 2013). Given the complexity of potential mechanisms driving oral repeat dose
85 toxicity, the current study employed the latter approach using the protocol described
86 hereafter.

87 *Structural similarity-based category formation*

88 All chemical structures were encoded as SMILES strings, neutralised and salts removed *prior*
89 to chemical similarity analysis. Structural similarity of each chemical to all others in the
90 dataset was calculated using the atom environments/Tanimoto coefficient approach as
91 implemented in the freely available Toxmatch software (V1.07). Categories were developed
92 for each chemical in the dataset using an in-house code implemented in Excel software that
93 identified analogues with a similarity index of 0.7 or greater. Categories containing three or
94 more chemicals were selected for further analysis.

95 *Structural alert-based category formation*

96 Each similarity-based category containing three or more chemicals was visually inspected in
97 order to identify key structural fragments present in all category members. This structural
98 fragment was then encoded as a SMARTS pattern-based structural alert. Each chemical in the
99 dataset was subsequently profiled against these structural alerts in order to expand the
100 groupings to include chemicals that were not found by the structural similarity analysis. This
101 is an important step in the protocol as pure structural similarity-based categories are
102 frequently unable to detect chemicals containing the key structural fragments. Structural
103 alerts were then subjected to a mechanistic analysis involving detailed literature work in
104 order to outline an MIE for the corresponding category members. This mechanistic analysis
105 involved establishing potential MIEs related to chronic toxicity and linking them to the

106 chemistry of the structural alerts. Structural alerts were only considered as robust if a clear
107 correlation between their chemistry and an MIE identified from relevant scientific literature
108 could be established.

109 *Development of a refined set of structural alerts and in silico profiler*

110 The final stage in the analysis was to use the mechanistic knowledge to extend the
111 applicability domain of the structural alerts enabling an *in silico* profiler to be developed.
112 This analysis involved identifying additional structural alerts capable of triggering the same
113 MIEs based on chemical information. The mechanistic rationale for these additional
114 structural alerts was supported by evidence drawn from the scientific literature. All structural
115 alerts identified in this study were then collated into an *in silico* profiler that allowed
116 chemicals capable of causing the same MIE to be assigned to a single category. In keeping
117 with the development of previous *in silico* profilers, the structural alerts were described
118 within the resulting *in silico* profiler based on commonality of the underlying chemistry.

119 Results and discussion

120 The aim of this study was to develop an *in silico* profiler suitable for chemical categorisation
121 of oral repeat dose toxicity data of hair dyes. The analysis involved utilising chemical
122 similarity to identify groups of chemicals from a dataset of 94 hair dyes. Data related to
123 repeat dose toxicity, as obtained from 90-day oral rat studies, were extracted from published
124 SCC(NF)P and SCCS opinions with NOAEL values ranging from 0.3 mg/kg/day up to 1000
125 mg/kg/day. The similarity analysis identified four categories of hair dyes containing either a
126 2-nitroaminobenzene, 4-nitroaminobenzene, aromatic azo or anthraquinone moieties. These
127 key structural fragments were used to develop a mechanistic hypothesis for the MIE for each
128 category. This analysis resulted in the definition of four structural alerts related to the ability
129 of aromatic chemicals to disrupt mitochondrial function due to their free radical chemistry.
130 This mechanistic chemistry allowed an *in silico* profiler containing a refined set of structural
131 alerts to be defined. The resulting *in silico* profiler assigned 56 of the 94 chemicals in the
132 dataset to a mechanism-based chemical category. However, further experimental analysis is
133 required to identify additional key steps to allow an AOP (or AOPs) to be defined.

134 *Development of mechanism-based structural alerts for category formation*

135 The chemo-informatics analysis identified four similarity-based categories in the dataset,
136 defined as a cluster containing three or more analogues. These included 2-
137 nitroaminobenzenes, 4-nitroaminobenzenes, aromatic azos and anthraquinones. In all
138 datasets, a structural alert was defined based on the key fragment in each of the clusters.
139 These structural alerts were used to identify additional related chemicals not identified by the
140 structural similarity analysis. This is a crucial step in the development of mechanism-based
141 structural alerts when using chemical similarity to cluster the initial dataset as related
142 chemicals are frequently omitted. The resulting structural alerts and the number of analogues
143 identified using them to re-analyse the data are summarised in Table 1.

144 [Table 1 here]

145 *2-nitroaminobenzene and 4-nitroaminobenzene structural alerts*

146 A total of 26 chemicals were identified using the 2-nitroaminobenzene and 4-
147 nitroaminobenzene structural alerts. The nitro group in these chemicals can be readily
148 reduced to an amino moiety by nitroreductase via a hydroxylamine intermediate in the gut
149 and the liver resulting in the production of 1,2- and/or 1,4-diaminobenzenes (Gorontzy *et al.*,
150 1993; Roldan *et al.*, 2008). These chemicals are then prone to oxidation to the corresponding
151 1,2- and/or 1,4-phenylenediamines (Figure 1).

152 [Figure 1 here]

153 Importantly, the conversion of 1,2-diaminobenzenes into 1,2-phenylenediamines is reversible
154 implying that these chemicals are capable of cycling electrons. This also holds true for the
155 corresponding 1,4-diaminobenzenes. It is known that this electron cycling mechanism allows
156 these types of chemicals to interfere with the electron transport chain within the mitochondria
157 (Wallace and Starkov, 2000). The mechanism leading to disruption could therefore involve
158 the 1,2-diaminobenzene moiety within a chemical accepting an electron from respiratory
159 complex I. This could oxidise the 1,2-diaminobenzene moiety to a 1,2-phenylenediamine
160 which thereafter could transport the electron several steps down the respiratory chain directly
161 into complex VI. The release of the electron would then reduce 1,2-phenylenediamine back
162 to a 1,2-diaminobenzene allowing the process to be repeated in a cyclic fashion (Figure 2).
163 This disruption ultimately could lead to a reduction in mitochondrial membrane potential and
164 a subsequent reduction in ATP production (Bironaite *et al.*, 1991; Chan *et al.*, 2005;
165 Munday, 1992; Wallace and Starkov, 2000).

166 [Figure 2 here]

167 The aromatic amine moiety of the reduction products is also known to induce uncoupling of
168 oxidative phosphorylation via a protonophoric mechanism (Terada, 1990) (Figure 3). The
169 deprotonated form of these compounds scavenges a free proton from the inner membrane
170 space. Upon protonation the compound is able to migrate across the inner mitochondrial
171 membrane into the mitochondrial matrix. Due to the increased alkaline environment within
172 the matrix the proton dissociates and the deprotonated compound returns to the inner
173 membrane space enabling the cycle to continue. The continuation of this cycle increases
174 oxygen consumption and heat production, alongside a reduction in the electrochemical
175 gradient and ATP production (Chan, Truong, Shangari and O'Brien, 2005; Pessayre *et al.*,
176 2012; Terada, 1990; Wallace and Starkov, 2000). Therefore, it is suggested that both
177 mechanisms might contribute to the observed mitochondrial dysfunction.

178 [Figure 3 here]

179 *Anthraquinone structural alert*

180 The structural alert based on the anthraquinone moiety identified a total of 5 chemicals in the
181 dataset. These chemicals have also been shown to be capable of disrupting the electron
182 transport chain in mitochondria by transporting electrons from respiratory complex I directly
183 to complex IV (Henry and Wallace, 1995; Kitani *et al.*, 1981). This process is similar to that
184 outlined for 1,2- and 1,4-diaminobenzenes in that the anthraquinone moiety accepts an
185 electron from complex I to become a semi-quinone radical. This radical species could
186 transport an electron directly to complex IV, being oxidised back to the anthraquinone in the
187 process (Figure 4). Again, this reaction is reversible allowing the anthraquinone moiety to
188 cycle electrons repeatedly from respiratory complex I to complex IV. In addition to acting as
189 direct electron transport agents, the production of the semi-quinone radical has also been
190 suggested to cause indirect mitochondrial toxicity due to their ability to react with molecular
191 oxygen to produce reactive oxygen species. The chemical species include hydroxyl and
192 superoxide radicals that are capable of evoking widespread damage to mitochondrial DNA,
193 proteins and lipids (Kappus, 1986; Ohkuma *et al.*, 2001).

194 [Figure 4 here]

195 *Aromatic azos structural alert*

196 The final structural alert identified from the similarity analysis related to chemicals
197 containing an aromatic azo moiety and identified 6 chemicals from the dataset. Chemicals
198 containing an aromatic azo linkage are readily reduced to the free amine by the enzyme
199 azoreductase (Nam and Renganathan, 2000). The presence of an additional nitro, amine or
200 hydroxyl group in the 2- or 4-position on at least one of the aromatic rings could result in the
201 possibility of the production of a 1,2- or 1,4-diaminobenzene moiety (Figure 5). This moiety
202 might then act as an electron cycling agent resulting in the disruption of the respiratory chain
203 in the mitochondria, as outlined previously for the 2-nitroaminobenzene and 4-
204 nitroaminobenzene clusters.

205 [Figure 5 here]

206 *Additional chemicals capable of electron cycling*

207 The mechanistic chemistry outlined for the four structural alerts identified from the similarity
208 analysis suggests that the ability to cycle electrons might represent a key MIE for
209 mitochondrial toxicity for aromatic chemicals of this type. The mechanistic analysis further
210 suggests that chemicals capable of forming free radicals could trigger this type of MIE
211 resulting in toxicity. Therefore, it should be possible to develop additional structural alerts
212 based around this mechanistic chemistry to increase the applicable chemical space relating to
213 the MIE with respect to electron cycling. For example, based on the analysis of the chemistry
214 outlined above for the 2-nitroaminobenzene category, it is conceivable to assume that
215 chemicals containing a 1,2-diaminobenzene moiety would also be capable of cycling
216 electrons, as this structure is one of the key intermediates in the mechanism proposed in
217 Figure 1. Table 2 defines a refined set of structural alerts of mechanistically related
218 chemicals. It should be noted, however, that the quinone structural alert includes chemicals
219 containing an anthraquinone moiety. The aromatic azo structural alert is included in Table 2
220 for completeness.

221 [Table 2 here]

222 The majority of the mechanistic chemistry for these structural alerts is as discussed
223 previously (Table 2). The scope of the pro-quinone structural alert is significantly extended as
224 evidenced by the number of chemicals assigned to the resulting category. This is due to the
225 extensive additional mechanistic chemistry knowledge in the wider literature relating to the
226 types of chemicals readily converted to the corresponding quinones (Enoch *et al.*, 2011b;

227 Kalgutkar *et al.*, 2005). In addition, the anthraquinone structural alert has been extended to
228 cover quinones, based on the related chemistry and the proven ability of these chemicals to
229 disrupt the respiratory chain in mitochondria via the same mechanism (Henry and Wallace,
230 1995; Kitani, So and Miller, 1981; Scatena *et al.*, 2007). In contrast, the mechanistic
231 chemistry for the three 1,3-substituted structural alerts is somewhat different to the remaining
232 structural alerts in that these chemicals are not able to form quinone-type species due to the
233 1,3-motif. However, it has been reported that they are capable of causing toxicity via a free
234 radical mechanism (Aptula *et al.*, 2009) (Figure 6). Thus, the inclusion of these three
235 structural alerts can be justified based on the hypothetical mechanistic rationale that a key
236 MIE for mitochondrial toxicity could be electron cycling due to free radical formation.

237 [Figure 6 here]

238 *Mitochondria and repeat dose toxicity*

239 The hypothetical mechanistic analysis presented above suggests that chemicals capable of
240 free radical chemistry might disrupt the respiratory chain in the mitochondria leading to
241 chronic toxicity. This is in keeping with previous research into the cardiotoxicity of
242 anthracyclines upon extended low dose exposure (Montaigne *et al.*, 2012). This adverse
243 reaction has been shown to be related to mitochondrial dysfunction which results in the
244 activation of a number of protein kinases. The MIE for this toxicity has been suggested to
245 involve the ability of the quinone moiety within these drugs to form a semi-quinone radical
246 and thus cycle electrons (Figure 3). In addition, these chemicals have been shown to form a
247 variety of reactive oxygen species also capable of disrupting the normal function of
248 mitochondria. It has also been suggested that mitochondrial dysfunction is a key driver in
249 chronic toxicity (Kovacic and Jacintho, 2001a; Kovacic and Jacintho, 2001b; Porceddu *et*
250 *al.*, 2012; Vinken, Whelan and Rogiers, 2013). A recent study also outlined how for the
251 same chemical the mechanism driving toxicity can change on-going from acute to chronic
252 exposure (Nikam *et al.*, 2013). The importance of mitochondrial dysfunction as a driver of
253 chronic toxicity has recently also led to the definition of a number of structural alerts, one of
254 which (2-aminonitrophenol) was included in the current study (Naven *et al.*, 2013).

255 [Table 3 here]

256 The data in Table 3 highlights that a variety of adverse effects within multiple organs are
257 associated with the NOAEL values for chemicals assigned to each category. This variability

258 in the toxicity profile adds weight to the hypothesis that the observed toxicity might have
259 been initiated by mitochondria dysfunction. This is due to the fact that mitochondria are
260 present within most organ systems, performing a number of roles vital to normal cellular
261 functioning. There is an extensive body of literature outlining a range of chemicals that
262 inhibit the mitochondrial physiology resulting in toxicity at the organ level (Dykens and Will,
263 2008). Typically, the most susceptible organs are those containing a higher concentration of
264 mitochondria, those exposed to a higher concentration of the compound and/or those with a
265 higher aerobic energy demand, such as the liver, kidney and cardiac muscle (Amacher, 2005;
266 Dykens and Will, 2008; Dykens and Will, 2007). In addition, it has been recognised by the
267 pharmaceutical industry that mitochondrial dysfunction may be a cause of numerous
268 toxicities within a variety of organs, and has led to the withdrawal of a number of therapeutic
269 drugs (Amacher, 2005; Dykens and Will, 2008; Dykens and Will, 2007; Pessayre,
270 Fromenty, Berson, Robin, Letteron, Moreau and Mansouri, 2012).

271 *Adverse Outcome Pathway concept, perspectives and proposed future work*

272 The analysis presented above outlines how structural alerts related to potential MIEs could
273 be derived. The main focus of this type of analysis is the development of the mechanistic
274 chemistry relating the structural alerts to a possible MIE. This focus is a process that involves
275 an in-depth survey of relevant scientific literature in support of the mechanistic hypothesis
276 made, enabling *in silico* profilers to be developed for a given MIE. The current study has
277 resulted in the development of a profiler capable of identifying chemicals that could cycle
278 electrons and thus lead potentially to the disruption of the respiratory chain in the
279 mitochondria. An important aspect of the on-going development of *in silico* profilers is the
280 experimental verification of the mechanistic hypothesis, which increases confidence in the
281 prediction of an MIE for an untested chemical. Such analysis has been recently undertaken
282 for the *in silico* profilers relating to covalent protein binding in the OECD QSAR Toolbox
283 (Enoch *et al.*, 2012b; Enoch *et al.*, 2013b; Nelms *et al.*, 2013; Rodriguez-Sanchez *et al.*,
284 2013). In terms of the current study, future work would consist of testing of a representative
285 number of hair dyes/chemicals from each of the categories outlined to cause mitochondrial
286 toxicity in an *in vitro* experimental set-up. In the longer term, the applicability domain of the
287 *in silico* profiler could then be much better defined through the use of directed and intelligent
288 testing of compounds using assays appropriately defined by the key events of the AOP.

289 To be able to predict oral repeat dose toxicity reliably, it is necessary, in addition to defining
290 the applicability domain of the *in silico* profiler and by extension the MIE associated with the
291 profiler, to generate extensive knowledge of subsequent key events in the AOP leading to
292 toxicity. This requirement is highlighted by the broad range of oral NOAEL values for the
293 categories derived in the current study which vary between one and two orders of magnitude
294 (Table 2 for the ranges, Table 3 for each chemical within each category). Importantly, these
295 values show the limitations of the *in silico* profilers ability to predict oral repeat dose toxicity.
296 Assuming no additional information is available, the most realistic prediction for an untested
297 chemical, assigned to one of the categories, would be to state that the oral NOAEL value
298 would be likely to fall within the range of the values for the other category members.
299 However, even this type of prediction may not be appropriate, in that the new untested
300 chemical could be capable of altering a downstream key event in the AOP in a different
301 manner to the remaining category members. It is also possible that the chemical may have a
302 different toxicokinetic and/or dynamic profile to the other category members. It is therefore
303 essential that the mechanistic information relating to the MIE contained within an *in silico*
304 profiler is complimented with information derived from other existing *in vivo* data, *in vitro*, *in*
305 *silico* or *in chemico* tests designed to target other key events in the AOP (and relating to
306 toxicokinetics and dynamics). Only when a significant proportion of this information is
307 available will the estimation of values such as NOAELs become possible without using
308 animal models.

309 Conclusions

310 This study proposes an *in silico* profiler for chemicals used as hair dyes capable of causing
311 mitochondrial dysfunction. It is based on a retrospective analysis of oral repeat dose toxicity
312 data for 94 hair dye chemicals and is intended for use in grouping and category formation. It
313 is important to note that the proposed profiler does not predict oral repeat dose toxicity;
314 instead it provides arguments for a key MIE that might be responsible for initiating an AOP
315 leading to chronic toxicity. This work generally shows that detailed mechanistic analysis is
316 required for the development of *in silico* profilers and explains how such analysis can be used
317 to identify potential MIEs. Clearly future *in vitro* work must be undertaken to outline
318 additional key events in biological pathway before a relevant and complete AOP could be
319 established.

320 Acknowledgements

321 The funding from the European Community's Seventh Framework Program (FP7/2007-2013)
322 COSMOS (grant agreement no 266835), HeMiBio (grant agreement no 266777) and
323 DETECTIVE (grant agreement no 266838) Projects, and from Cosmetics Europe is gratefully
324 acknowledged. See cosmostox.eu, hemibio.eu and detect-iv-e.eu for more details.

325 Conflicts of interest statement

326 The authors declare that there are no conflicts of interest.

327 References

- 328 Commission, E. (2003). Directive 2003/15/EC (Cosmetics Directive) *Official Journal of the European*
329 *Union*.
- 330 Commission, E. (2007). REACH technical guidance (located at <http://ecb.jrc.it/reach/rip/>) In (
331 Ankley, G. T., Bennett, R. S., Erickson, R. J., Hoff, D. J., Hornung, M. W., Johnson, R. D., Mount, D. R.,
332 Nichols, J. W., Russom, C. L., Schmieder, P. K., Serrano, J. A., Tietge, J. E., and Villeneuve, D. L. (2010).
333 Adverse outcome pathways: A conceptual framework to support ecotoxicology research and risk
334 assessment. *Environmental Toxicology and Chemistry* **29**(3), 730-741.
- 335 Vinken, M. (2013). The adverse outcome pathway concept: A pragmatic tool in toxicology.
336 *Toxicology* **312**, 158-165.
- 337 Vinken, M., Whelan, M., and Rogiers, V. (2013). Adverse outcome pathways: hype or hope? *Archives*
338 *of Toxicology* **Guest editorial**.
- 339 Przybylak, K. R., and Schultz, T. W. (2013). Informing Chemical Categories through the Development
340 of Adverse Outcome Pathways. In *Chemical Toxicity Prediction: Category Formation and Read-Across*
341 (M. T. D. Cronin, J. C. Madden, S. J. Enoch, and D. W. Roberts, Eds.), Vol. 17, pp. 44-71. RSC,
342 Cambridge, UK.
- 343 Enoch, S. J., Cronin, M. T. D., and Ellison, C. M. (2011a). The use of a chemistry based profiler for
344 covalent DNA binding in the development of chemical categories for read-across for genotoxicity.
345 *ATLA-Alternatives to Laboratory Animals* **39**, 131-145.
- 346 Enoch, S. J., Przybylak, K. P., and Cronin, M. T. D. (2013a). Category Formation Case Studies. In
347 *Chemical Toxicity Prediction: Category Formation and Read-Across* (M. T. D. Cronin, J. C. Madden, S.
348 J. Enoch, and D. W. Roberts, Eds.), Vol. 17. RSC, Cambridge, UK.
- 349 Enoch, S. J., and Roberts, D. W. (2013). Approaches for grouping chemicals into categories. In
350 *Chemical Toxicity Prediction: Category Formation and Read-Across* (M. T. D. Cronin, J. C. Madden, S.
351 J. Enoch, and D. W. Roberts, Eds.), pp. 30-43. The Royal Society of Chemistry, Cambridge, UK.
- 352 Sakuratani, Y., Zhang, H. Q., Nishikawa, S., Yamazaki, K., Yamada, T., Yamada, J., Gerova, K., Chankov,
353 G., Mekenyan, O., and Hayashi, M. (2013a). Hazard Evaluation Support System (HESS) for predicting
354 repeated dose toxicity using toxicological categories. *SAR and QSAR in Environmental Research* **24**,
355 351-363.
- 356 Sakuratani, Y., Zhang, H. Q., Nishikawa, S., Yamazaki, K., Yamada, T., Yamada, J., and Hayashi, M.
357 (2013b). Categorization of nitrobenzenes for repeated dose toxicity based on adverse outcome
358 pathways. *SAR and QSAR in Environmental Research* **24**, 35-46.
- 359 Gutsell, S., and Russell, P. (2013). The role of chemistry in developing understanding of adverse
360 outcome pathways and their application in risk assessment. *Toxicology Research* **2**, 299-307.
- 361 Gago-Dominguez, M., Castelao, J. E., Yuan, J., Yu, M. C., and Ross, R. K. (2001). Use of permanent hair
362 dyes and bladder cancer risk. *International Journal of Cancer* **91**, 575-579.
- 363 Enoch, S. J., Cronin, M. T. D., Schultz, T. W., and Madden, J. C. (2008). Quantitative and mechanistic
364 read across for predicting the skin sensitisation potential of alkenes acting via Michael addition.
365 *Chemical Research in Toxicology* **21**, 513-520.

366 Enoch, S. J., Seed, M. J., Roberts, D. W., Cronin, M. T. D., Stocks, S. J., and Agius, R. M. (2012a).
367 Development of mechanism-based structural alerts for respiratory sensitisation hazard
368 identification. *Chemical Research in Toxicology* **25**, 2490-2498.

369 Hewitt, M., Enoch, S. J., Madden, J. C., Przybylak, K. P., and Cronin, M. T. D. (2013). Hepatotoxicity: A
370 scheme for generating chemical categories for read-across, structural alerts and insights into
371 mechanism(s) of action *Critical Reviews in Toxicology* **43**(7), 537-558.

372 Gorontzy, T., Kuver, J., and Blotevogel, K. (1993). Microbial transformation of nitroaromatic
373 compounds under anaerobic conditions. *Journal of General Microbiology* **139**, 1331-1336.

374 Roldan, M. D., Perez-Reinado, E., Castillo, F., and Moreno-Vivian, C. (2008). Reduction of
375 polynitroaromatic compounds: the bacterial nitroreductases. *Microbiology Reviews* **32**, 474-500.

376 Wallace, K. B., and Starkov, A. A. (2000). Mitochondrial targets of drug toxicity. *Annual Reviews of*
377 *Pharmacology and Toxicology* **40**, 353-388.

378 Bironaite, D. A., Cenas, N. K., and Kulys, J. (1991). The rotenone-insensitive reduction of quinones
379 and nitrocompounds by mitochondrial NADH: ubiquinone reductase. *Biochemica et Biophysica Acta*
380 **1060**, 203-209.

381 Chan, K., Truong, D., Shangari, N., and O'Brien, P. J. (2005). Drug-induced mitochondrial toxicity.
382 *Expert Opinion in Drug Metabolism and Toxicology* **1**, 655-669.

383 Munday, R. (1992). Mitochondrial oxidation of p-phenylenediamine derivatives in vitro: Structure-
384 activity relationships and correlation with myotoxic activity in vivo. *Chemico-Biological Interactions*
385 **82**, 165-179.

386 Terada, H. (1990). Uncouplers of oxidative phosphorylation. *Environmental Health Perspectives* **87**,
387 213-218.

388 Pessayre, D., Fromenty, B., Berson, A., Robin, M., Letteron, P., Moreau, R., and Mansouri, A. (2012).
389 Central role of mitochondria in drug-induced liver injury. *Drug Metabolism Reviews* **44**, 34-87.

390 Henry, T. R., and Wallace, K. B. (1995). Differential mechanisms of induction of the mitochondrial
391 permeability transition by quinones of varying chemical reactivities. *Toxicology and Applied*
392 *Pharmacology* **134**, 195-203.

393 Kitani, A., So, Y., and Miller, L. L. (1981). An electrochemical study of the kinetics of NADH being
394 oxidised by diimines derived from diaminobenzenes and diaminopyrimidines. *Journal of the*
395 *American Chemical Society* **103**, 7636-7641.

396 Kappus, H. (1986). Overview of enzyme systems involved in bio-reduction of drugs and in redox
397 cycling. *Biochemical Pharmacology* **335**, 1-6.

398 Ohkuma, Y., Hiraku, Y., and Kawanishi, S. (2001). Sequence-specific DNA damage induced by
399 carcinogenic danthron and anthraquinone in the presence of Cu(II), cytochrome P450 reductase and
400 NADPH. *Free Radical Research* **34**, 595-604.

401 Nam, S., and Renganathan, V. (2000). Non-enzymatic reduction of azo dyes by NADH. *Chemosphere*
402 **40**, 351-357.

403 Enoch, S. J., Ellison, C. M., Schultz, T. W., and Cronin, M. T. D. (2011b). A review of the electrophilic
404 reaction chemistry involved in covalent protein binding relevant to toxicity. *Critical Reviews in*
405 *Toxicology* **41**, 783-802.

406 Kalgutkar, A. S., Gardner, I., Obach, R. S., Shaffer, C. L., Callegari, E., Henne, K. R., Mutlib, A. E.,
407 Dalvie, D. K., Lee, J. S., Nakai, Y., O'Donnell, J. P., Boer, J., and Harriman, S. P. (2005). A
408 comprehensive listing of bioactivation pathways of organic functional groups. *Current Drug*
409 *Metabolism* **6**, 161-225.

410 Scatena, R., Bottoni, P., Botta, G., Martorana, G. E., and Giardina, B. (2007). The role of mitochondria
411 in pharmacotoxicology: A re-evaluation of an old, newly emerging topic. *American Journal of*
412 *physiology and Cell Physiology* **293**, C12-C21.

413 Aptula, A. O., Enoch, S. J., and Roberts, D. W. (2009). Chemical mechanisms for skin sensitisation by
414 aromatic compounds with hydroxy and amino groups. *Chemical Research in Toxicology* **22**, 1541-
415 1547.

416 Montaigne, D., Hurt, C., and Nevriere, R. (2012). Mitochondria death/survival signalling pathways in
417 cardiotoxicity induced by anthracyclines and anticancer-targeted therapies. *Biochemistry Research*
418 *International* **2012**, ID 951539.

419 Kovacic, P., and Jacintho, J. D. (2001a). Mechanisms of carcinogenesis: Focus on oxidative stress and
420 electron transfer. *Current Medicinal Chemistry* **8**, 773-796.

421 Kovacic, P., and Jacintho, J. D. (2001b). Reproductive toxins: Pervasive theme of oxidative stress and
422 electron transfer. *Current Medicinal Chemistry* **8**, 863-892.

423 Porceddu, M., Buron, N., Roussel, C., Labbe, G., Fromenty, B., and Borgne-Sanchez, A. (2012).
424 Prediction of liver injury induced by chemicals in human with a multiparametric assay on isolated
425 mouse liver mitochondria. *Toxicological Sciences* **129**, 332-345.

426 Nikam, A., Patankar, J. V., Lackner, C., Schock, E., Kratky, D., Zatloukal, K., and Abuja, P. M. (2013).
427 Transition between acute and chronic hepatotoxicity in mice is associated with impaired energy
428 metabolism and induction of mitochondrial heam oxygenase-1. *PLoS ONE* **8**, e66094.

429 Naven, R. T., Swiss, R., Klug-Mcleod, J., Will, Y., and Greene, N. (2013). The development of
430 structure-activity relationships for mitochondrial dysfunction: Uncoupling of oxidative
431 phosphorylation. *Toxicological Sciences* **131**(1), 271-278.

432 Dykens, J. A., and Will, Y. (2008). *Drug-induced mitochondrial dsyfunction*. Wiley-Interscience, New
433 Jersey, USA.

434 Amacher, D. E. (2005). Drug-associated mitochondrial toxicity and its detection. *Current Medicinal*
435 *Chemistry* **12**, 1829-1839.

436 Dykens, J. A., and Will, Y. (2007). The signifcance of mitochondrial toxicity testing in drug
437 development. *Drug Discovery Today* **12**, 777-785.

438 Enoch, S. J., Cronin, M. T. D., and Schultz, T. W. (2012b). The definition of the applicability domain
439 relevant to skin sensitisation for the aromatic nucleophilic substitution electrophilic mechanism. *SAR*
440 *and QSAR in Environmental Research* **23**, 649-663.

441 Enoch, S. J., Cronin, M. T. D., and Schultz, T. W. (2013b). The definition of the toxicologically relevant
442 applicability domain for the S_NAr reaction for substituted pyridines and pyrimidines. *SAR and QSAR in*
443 *Environmental Research* **24**, 385-392.

444 Nelms, M. D., Cronin, M. T. D., Schultz, T. W., and Enoch, S. J. (2013). Experimental verification, and
445 domain definition, of structural alerts for protein binding: epoxides, lactones, nitroso, nitros,
446 aldehydes and ketones. *SAR and QSAR in Environmental Research* **24**, 695-709.

447 Rodriguez-Sanchez, N., Schultz, T. W., Cronin, M. T. D., and Enoch, S. J. (2013). Experimental
448 verification of structural alerts for the protein binding of cyclic compounds acting as Michael
449 acceptors. *SAR and QSAR in Environmental Research* **in press**.

450

451

452 Figure 1: Reduction of 2-nitroaminobenzene to the corresponding 1,2-diaminobenzene and
453 then subsequent oxidation to a 1,2-phenylenediamine

454 Figure 2: Electron cycling process leading to disruption of the respiratory chain in the
455 mitochondria due to the presence of an alternate electron acceptor

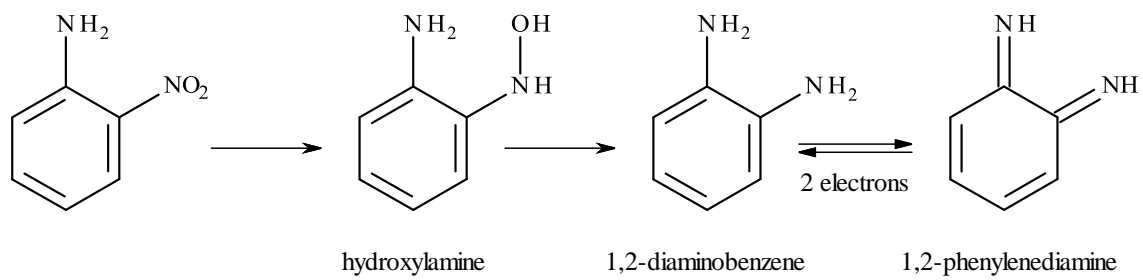
456 Figure 3: Cycling of the compound within the inner membrane space (IMM), scavenging
457 hydrogen ions from within the inner membrane space (IMS) and transporting them to the
458 mitochondrial matrix (MM)

459 Figure 4: Activation of the anthraquinone moiety into a semi-quinone radical

460 Figure 5: Reduction of aromatic azo compounds producing a 1,4-diaminobenzene and 1,4-
461 phenylenediamine capable of cycling electrons

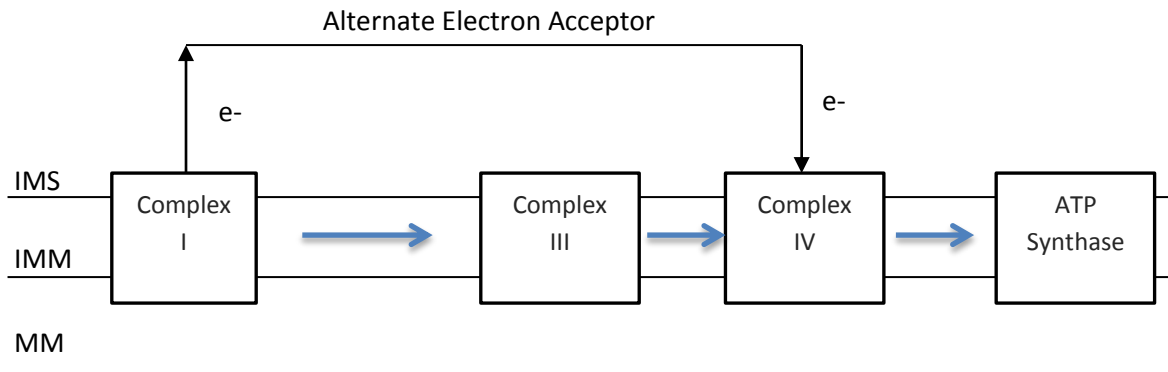
462 Figure 6: Free radical mechanism for 1,3-diaminobenzene (an analogous mechanism is
463 possible for the 1,3-dihydroxybenzene and 3-hydroxyaminobenzene containing chemicals)

464



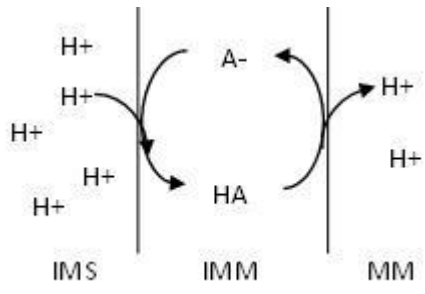
465

466



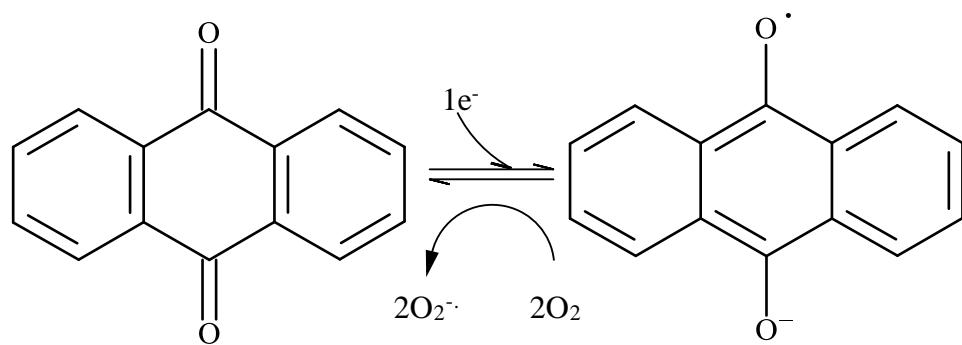
467

468



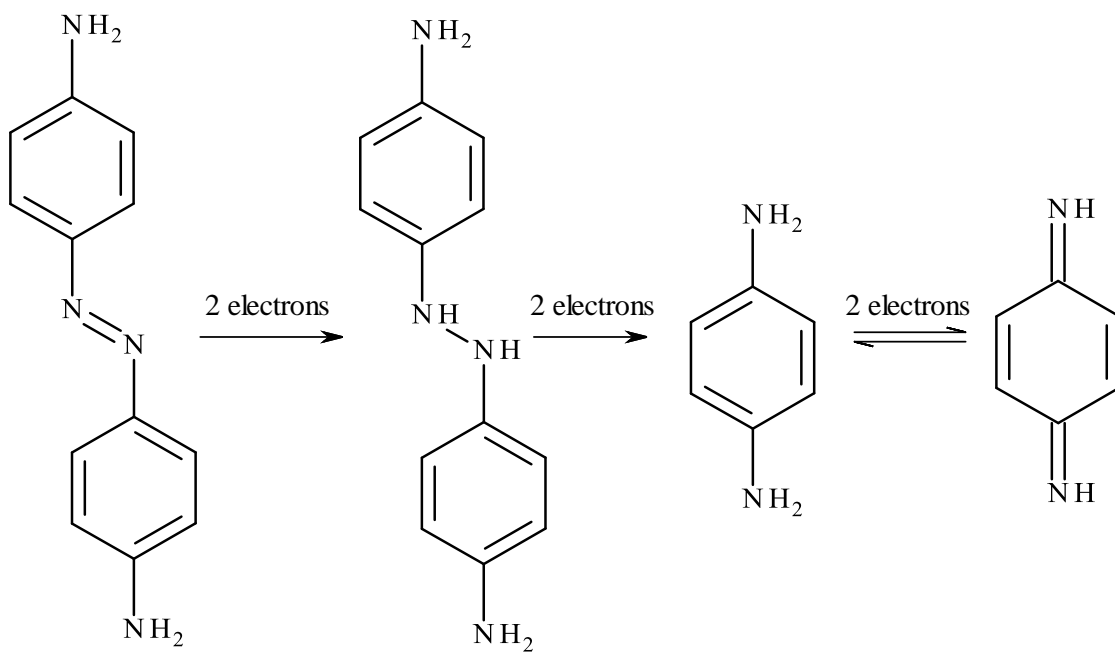
469

470



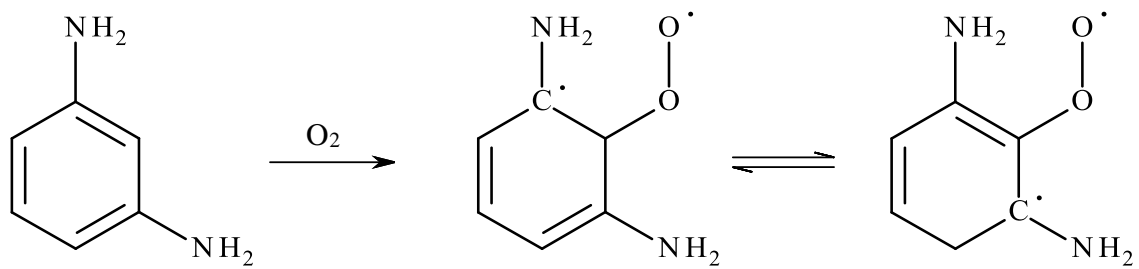
471

472



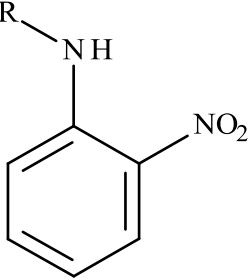
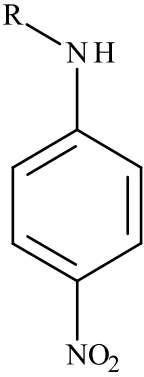
473

474



475

476 Table 1: Structural alerts identified from the similarity analysis carried out on the 93 hair dye
 477 chemicals

Structural alert	Key structural fragment	Number of analogues
2-nitroaminobenzenes	 <p>R = hydrogen, carbon</p>	20
4-nitroaminobenzenes	 <p>R = hydrogen, carbon</p>	6

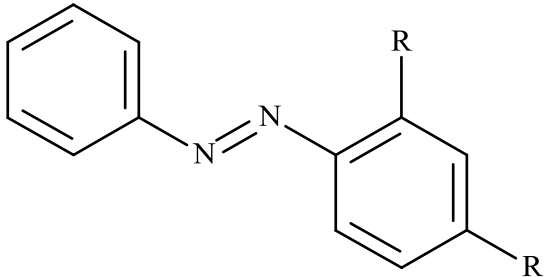
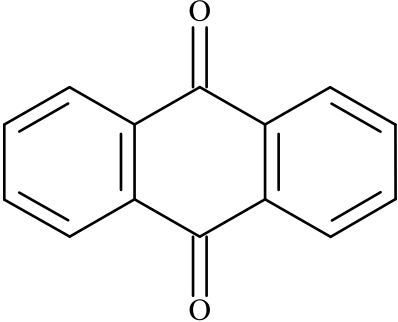
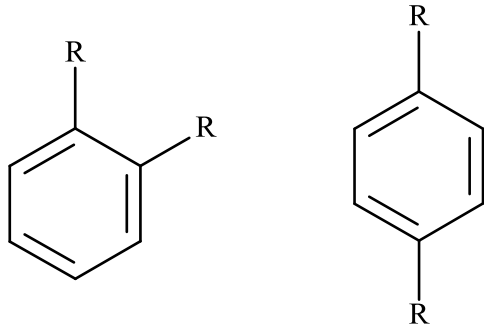
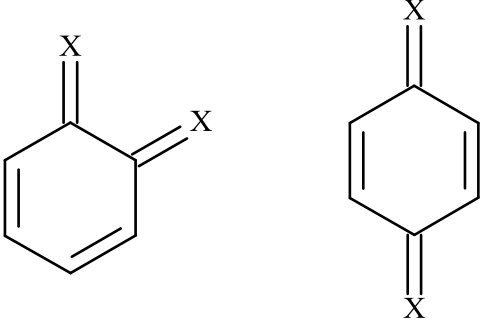
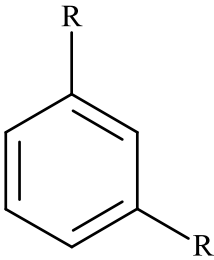
<p>Aromatic azos</p>	 <p>R = at least must be NH₂, NH</p>	<p>6</p>
<p>Anthraquinones</p>		<p>5</p>

Table 2: Refined set of structural alerts capable of free radical cycling chemistry (NOAEL values relate to 90-day oral rat studies)

Name	Key structural features	Number of chemicals	oral NOAEL ranges (mg/kg/day)	Figure
Pro-quinones (R = OH, NH ₂ , NH, NO ₂)	 <p>The image shows two chemical structures of substituted benzene rings. The first structure is a benzene ring with two 'R' groups attached at the 1 and 2 positions (ortho-substitution). The second structure is a benzene ring with two 'R' groups attached at the 1 and 4 positions (para-substitution).</p>	39	1.4 – 250.0	1

<p>Quinones (X = NH, O)</p>		<p>7</p>	<p>2.0 – 200.0</p>	<p>3</p>
<p>Meta-substituted benzenes (R = NH₂, OH)</p>		<p>4</p>	<p>50.0 – 100.0</p>	<p>5</p>

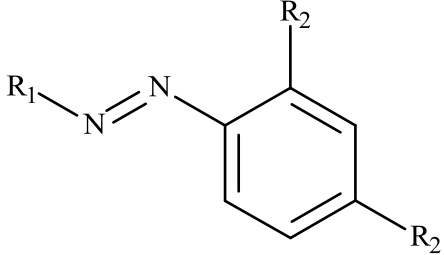
<p>Aromatic azos $(R_1 = \text{aromatic carbon})$ $(R_2 = \text{NH}_2, \text{NH}, \text{OH})$</p>		<p>6</p>	<p>0.3 – 52.6</p>	<p>4</p>
---	--	----------	-------------------	----------

Table 3: Repeat dose data the chemicals grouped into categories by the structural alerts defined in the current study (AAT – alanine aminotransferase, APTT – activated partial thromboplastin time, AST – aspartate aminotransferase, BWG – body weight gain, GI – gastrointestinal, MCH – Mean Corpuscular/cell Haemoglobin, MCV – Mean Corpuscular/cell Volume, PT – Prothrombin Time, RBC – Red Blood Cell)

ID	Category	Chemical	NO(A)EL (mg/kg bw/day)	LO(A)EL (mg/kg bw/day)	Reported adverse effects
1	Quinone	Disperse Violet 1	2	20	<ul style="list-style-type: none"> ↑ Centrilobular/Midzonal hepatocyte hypertrophy ↑ Triglycerides (♀) ↑ Cholesterol ↓ Motor activity
2	Quinone	Lawsone	2	7	<ul style="list-style-type: none"> ↓ Erythrocyte count (♀) ↓ Blood urea (♀) ↓ Albumin:Globulin ratio (♀) ↑ Bilirubin (♀) ↑ Kidney weight (♀) ↓ Blood glucose (♂) ↑ Triglycerides (♂) ↑ Haematopoiesis, spleen (♂) ↑ (Multi)focal ulceration of mucosa, forestomach ↑ Interstitial oedema, forestomach
3	Quinone	Acid Green 25	100	300	<ul style="list-style-type: none"> ↑ Kidney weight
4	Quinone	HC Green No. 1	100	300	<ul style="list-style-type: none"> ↓ Food consumption (♀) ↓ Body weight (♀) ↑ Hypokalemia ↑ Oliguria (♂)
5	Quinone	Acid Blue 62	300	1000	<ul style="list-style-type: none"> ↑ Kidney weight ↑ Liver weight

					<ul style="list-style-type: none"> ↑ Ptyalism ↑ Tubular nephrosis ↑ Centrilobular hepatocyte hypertrophy ↑ Blood Urea ↑ Albumin ↑ Cholesterol ↑ AAT ↓ Body weight ↓ Glucose
6	Quinone	Hydroxyanthraquinone aminopropyl methyl morpholinium methosulfate	200	800	<ul style="list-style-type: none"> ↓ Absolute thymus weight (♀) ↓ Body weight (♂) ↓ Relative thymus weight
7	Quinone	Acid Violet 43	300	1000	<ul style="list-style-type: none"> ↑ PT ↑ APTT
8	Pro-quinone	Toluene-2,5-diamine	10	20	<ul style="list-style-type: none"> ↑ AST ↑ Mononuclear cell infiltrates, diaphragm ↑ Mononuclear cell infiltrates, eye ↑ Mononuclear cell infiltrates, thigh ↑ Mononuclear cell infiltrates, tongue ↑ Muscular degeneration, diaphragm ↑ Muscular degeneration, thigh ↑ Muscular degeneration, tongue ↑ Muscular regeneration, diaphragm
9	Pro-quinone	Picramic acid	5	15	<ul style="list-style-type: none"> ↑ Ulceration of GI tract ↑ Inflammation of GI tract ↑ Fibrosis of GI tract ↑ Tubular cell swelling ↑ MCV ↑ MCH ↑ Reticulocyte count
10	Pro-quinone	HC Red No. 13	No NO(A)EL	5	<ul style="list-style-type: none"> ↑ Creatinine (♀)

					↑ Kidney weight ↑ PT (♂) ↓ Albumin:Globulin ratio (♀) ↓ Glucose (♀) ↓ MCH (♂) ↓ MCV
11	Pro-quinone	2,2'-Methylenebis-4-aminophenol	5	15	↑ Cast formation, kidney ↑ Thickened basement membrane, kidney ↑ Tubular basophilia, kidney ↑ Tubular degeneration, kidney
12	Pro-quinone	4-Nitrophenyl aminoethylurea	5	25	↓ RBC count ↓ Haemoglobin concentration ↑ MCV ↑ Reticulocyte count ↑ Extramedullary haematopoiesis, spleen ↑ Haemosiderosis (♀) ↓ Packed cell volume (♂)
13	Pro-quinone	HC Red No. 1	5	20	↓ Erythrocytes (♀) ↑ Leukocytes (♀) ↑ Lymphocytes (♀) ↓ Thymus weight (♂) ↑ MCH (♂)
14	Pro-quinone	Tetrahydro-6-nitroquinoxaline	5	25	↑ Ptyalism ↑ Liver weight ↑ Spleen weight
15	Pro-quinone	p-Phenylenediamine	8	16	↑ Myodegeneration, skeletal muscle
16	Pro-quinone	2-Chloro-6-ethylamino-4-nitrophenol	10	30	↑ Liver weight
17	Pro-quinone	Dihydroxyindoline	10	20	↑ Pigmentation, kidney
18	Pro-quinone	PEG-3-2',2'-di-p-phenylenediamine	10	25	↑ Intracellular pigmentation, kidney tubules ↑ Pigmentation, thyroid epithelium ↑ Pigmentation, duodenum

19	Pro-quinone	p-Methylaminophenol sulphate	10	30	<ul style="list-style-type: none"> ↑ Tubular epithelial degeneration, kidney ↑ Single cell necrosis, kidney ↓ Specific gravity (♂) ↑ Urinary volume (♂)
20	Pro-quinone	2-Hydroxyethyl picramic acid	15	60	<ul style="list-style-type: none"> ↑ Protein cylinders, kidneys ↑ Activation of thyroid epithelial cells
21	Pro-quinone	HC Yellow No. 13	21	90	<ul style="list-style-type: none"> ↑ Degeneration, Islet cells ↑ Inflammation, endocrine pancreas ↑ Fibrosis, endocrine pancreas ↑ Serum cholesterol (♂)
22	Pro-quinone	3-Methylamino-4-nitrophenoxyethanol	25	100	<ul style="list-style-type: none"> ↑ Ptyalism ↓ Lymphoid in thymus
23	Pro-quinone	HC Orange No.1	25	No LO(A)EL	Nothing reported
24	Pro-quinone	2-Amino-6-chloro-4-nitrophenol	30	90	<ul style="list-style-type: none"> ↓ Body weight ↑ Kidney weight
25	Pro-quinone	4-Hydroxypropylamino-3-nitrophenol	30	90	<ul style="list-style-type: none"> ↑ Thyroid weight ↓ AST
26	Pro-quinone	Acid Yellow 1	30	100	<ul style="list-style-type: none"> ↑ Mean absolute reticulocyte ↑ Haematopoiesis ↑ Lesions, caecum ↑ Lesions, intestine ↑ Lesions, liver ↑ Lesions, spleen ↑ Haemosiderosis (♀) ↑ MCV (♀) ↑ Spleen weight (♂)
27	Pro-quinone	1,2,4-Trihydroxybenzene	50	100	<ul style="list-style-type: none"> ↑ Piloerection ↑ Ptyalism ↑ Mean RBC volume ↑ MCH ↑ Platelets ↓ Haematocrit

					↓ RBC count ↓ Haemoglobin ↑ Kidney weight ↑ Liver weight ↑ Spleen weight ↓ Body weight (♂)
28	Pro-quinone	4-Amino-3-nitrophenol	50	250	↑ Liver weight (♂)
29	Pro-quinone	HC Violet No. 2	50	200	↑ Liver weight ↓ RBC ↓ PT
30	Pro-quinone	HC Yellow No. 11	50	200	↑ Acidophilic globules in cortical tubular epithelium ↑ Liver weight (♀) ↑ Kidney weight ↓ Thymus weight ↓ Creatinine
31	Pro-quinone	HC Yellow No. 2	50	No LO(A)EL	Nothing reported
32	Pro-quinone	2-Nitro-4-amino-diphenylamine-2'-carboxylic acid	60	180	↑ Thrombocytes ↑ Water consumption (♀)
33	Pro-quinone	4-Amino-m-cresol	60	120	↑ Spleen weight
34	Pro-quinone	HC Blue No. 12	60	No LO(A)EL	Nothing reported
35	Pro-quinone	HC Blue No. 11	80	160	↑ Kidney weight ↑ Vacuolated tubular cell
36	Pro-quinone	HC Red No. 3	90	250	↓ Body weight
37	Pro-quinone	2-Hydroxyethylamino-5-nitroanisole	100	500	↑ Liver weight ↑ Spleen weight ↑ PT ↑ Fibrinogen level ↑ Blood urea nitrogen ↑ AAT (♂) ↑ Urinary volume

38	Pro-quinone	HC Orange No. 3	100	300	<ul style="list-style-type: none"> ↑ Kidney weight ↑ Liver weight ↑ Spleen weight ↑ AAT ↑ AST
39	Pro-quinone	HC Yellow No. 10	100	500	<ul style="list-style-type: none"> ↑ Staining, body ↑ Staining, fur ↑ Body weight ↑ Ptyalism ↑ Food consumption ↑ Liver weight ↑ Spleen weight (♂)
40	Pro-quinone	HC Orange No. 2	150	500	<ul style="list-style-type: none"> ↑ Ptyalism ↓ BWG ↓ Food consumption ↓ Blood glucose
41	Pro-quinone	Acid Blue 62	300	1000	<ul style="list-style-type: none"> ↑ Kidney weight ↑ Liver weight ↑ Ptyalism ↑ Tubular nephrosis ↑ Centrilobular hepatocyte hypertrophy ↑ Blood urea ↑ Albumin ↑ Cholesterol ↑ AAT ↓ BWG ↓ Glucose
42	Pro-quinone	2-Nitro-5-glyceryl methylaniline	200	800	<ul style="list-style-type: none"> ↑ Ptyalism ↑ Vacuolated pancreatic cells ↑ Vacuolated renal tubular cells ↑ Tubular nephrosis ↑ Piloerection

					↑ Hunched back ↑ Hypokinesia ↑ Bilateral opacity ↑ Adrenal weight ↑ Kidney weight ↑ Liver weight ↓ BWG
43	Pro-quinone	3-Nitro-p-hydroxyethylaminophenol	200	No LO(A)EL	Nothing reported
44	Pro-quinone	N,N'-bis(hydroxyethyl)-2-nitro-p-phenylenediamine	240	720	↑ Kidney weight ↑ Liver weight ↓ Activity (♀) ↓ Ataxia (♀) ↑ Ptyalism (♀) ↑ Ocular discharge (♀) ↑ Lethargy (♀) ↑ Hunched posture (♀) ↑ Triglycerides (♂) ↑ Urea (♂) ↑ Urinary specific gravity
45	Pro-quinone	HC Yellow No. 4	250	500	↓ Body weight ↑ Thyroid lesions ↑ Uterine lesions (♀) ↑ Kidney lesions (♂) 1 Mortality
46	Pro-quinone	HC Yellow No. 9	250	No LO(A)EL	Nothing reported
47	Meta-hydroquinone	5-amino-6-chloro-o-cresol	No NO(A)EL	100	↑ Centrilobular hepatotrophy, liver ↑ MCV ↑ Mean corpuscular Hb (♀) ↑ MCH concentration (♀)
48	Meta-hydroquinone	3-Amino-2,4-dichlorophenol	80	160	↑ Liver degeneration ↑ Liver necrosis

					↑ Foci mononuclear cell infiltration ↑ Kidney degeneration ↑ Kidney necrosis ↑ Tubular epithelial cell hypertrophy ↑ Phosphorus (♂) ↑ Sodium (♂) ↑ Chloride (♂)
49	Meta-hydroquinone	2,6-Dihydroxyethylaminotoluene	100	316	↑ Bilirubin ↑ Urobilinogen ↓ Serum creatinine (♀)
50	Meta-hydroquinone	2-Methylresorcinol	100	200	↑ Clonic spasms ↑ Ptyalism ↑ Scratching movements ↑ Body weight (♂) ↑ Liver weight (♂) ↑ AST (♂) ↑ AAT (♂)
51	Aromatic azo	Basic Brown 16	50	150	↓ BWG (M)
52	Aromatic azo	Basic Brown 17	60	120	↑ Extramedullary haemopoiesis
53	Aromatic azo	Basic Red 76	20	60	↓ RBC (M) ↓ Haemoglobin ↓ Haematocrit (M) ↓ MCH concentration (F)
54	Aromatic azo	Disperse Black 9	100	No LO(A)EL	Nothing reported
55	Aromatic azo	Disperse Red 17	10	30	↑ Spleen weight
56	Aromatic azo	HC Yellow N°. 7	10	40	↑ Kidney weight ↑ Bilateral discolouration of fundus ↑ Ptyalism ↑ Tubular basophilia ↑ Blood phosphorous (F) ↓ Blood glucose (F) ↑ Blood sodium (M)

